Squirrel Cage Induction Motor Design and the Effect of Specific Magnetic and Electrical Loading Coefficient

Asım Gökhan Yetgin[*,1], Mustafa Turan[2], Barış Cevher[2], Ali İhsan Çanakoğlu[3], Ayhan Gün[3]

Abstract: 3-phase induction motors are widely used in industrial applications such as pumps, blowers, compressors, conveyors, etc. In addition, single-phase motors also have domestic use. For this reason, the design of the induction motor is of great importance. During the design, according to the parameters given as input, there are many situations that are contradictory to each other in order to achieve the goal. For example, if high efficiency is required, the motor size and the price will increase, and if lower price is required, other performance characteristics should be ignored. In the practical design of an induction motor, the designer has to comply with a number of constraints because of the large number of input variables. For this reason manual calculation becomes a very long and difficult process. To overcome this tiresome process, it is necessary to create a computer aided program or simulation model to determine the induction motor design parameters. In induction motor design, many parameters directly affect motor performance. Therefore, the selection of these parameters is of great importance. The output coefficient (C_0), which takes place in the first steps of the design process, also has a great influence on the motor design. In this paper, a program for optimizing design of 3-phase induction motors written in MATLAB is presented. The structure of the program is modular and therefore can be modified for the various requirements of the induction motor design. C_0 constant, one of the design parameters, also varies with some other parameters. The most important ones are the specific electrical loading coefficient (A_1) and the specific magnetic loading coefficient (B_{av}), making dramatic effect on the output coefficient. The effect of the variation of the C_0 constant on the performance of the induction motor was investigated in the study. Stator inner and outer diameter, stack length, stator and rotor slot parameters, equivalent circuit parameters, losses and efficiency was obtained according to the change of B_{av} and A_1 values. The obtained results are given and interpreted in tables and graphs.

Keywords: *Electrical loading coefficient, Induction motor design, Magnetic loading coefficient, Output coefficient, Performance analysis.*

1. Introduction

Induction machines, which have the most widespread use in today's industry, are usually manufactured as single or three-phase motors. This machines are widely used in various fields ranging from home applications to space technology. For this reason, design of the motor is of great importance in practice. During design, there are many inconsistent situations that are contradictory to each other in order to achieve the desired result according to the given characteristics. For example, if high efficiency is required, the motor size will increase and the price will increase. If lower prices are required, other performance requirements are ignored. While induction motors are examined, the effects of fundamental variables on motor performance are found by using magnetic, electric and thermal models. In the design of induction motors, motor geometry and winding types which are effective in desired performance values are determined. The obtained model in design includes magnetic and electrical models [1].

The main specifications for the design of a three phase squirrel cage induction motor are: rated output power, frequency, voltage, speed, efficiency, power factor and full load current etc. The standard specification for the design of an induction motor are materials (lamination thickness, conductor diameter), performance indexes (efficiency, power factor, starting torque, starting current, breakdown torque), temperature by insulation class, frame sizes, shaft height, cooling types, service classes, protection classes, etc.

are specified in national (or international) standards (NEMA, IEEE, IEC, EU, etc.) to facilitate the induction motor for various applications. The main purpose of designing an induction motor is to obtain the complete physical dimensions of all the parts of the machine as mentioned below to satisfy the given specifications [2].
- The main dimensions of the stator
- Details of stator and stator windings
- Design details of rotor and its windings
- Performance characteristics (Iron losses, copper losses, efficiency, no load current, power factor) [3]

The stator and rotor dimensions are determined by independent variables which are: stator slot height, stator tooth width, rotor slot height, rotor tooth width, air-gap length, air gap flux density, stack length, outer stator diameter, stator wire size and electrical steel type. Besides the above independent variables, the design involves some non-linear constraints which concern mainly the motor performances. They are stator winding temperature, rotor bar temperature, flux density in the stator. The type of winding adopted in this design is the squirrel cage type as it is simpler and economical, which consists of a number of bars embedded in the rotor slots and connected at both ends by means of end rings [2].

In this study, the design processes of a 3 phase squirrel cage induction motor are discussed and a sample design is given. In addition, the effects of specific electric loading coefficient and specific magnetic loading coefficients were analysed in the design process which were not taken into consideration but which significantly affected the performance of the motor values. The effects of these two coefficients on motor performance were

investigated. The inner diameter, outer diameter, package length, stator and rotor slot geometries, the change of the equivalent circuit parameters, losses and the change of the efficiency values of the motor were examined.

2. Design Procedure of Induction Motor

Wengerkievicz et al. proposed 5 different methods for the determination of induction motor parameters [4].

1. Calculation from construction data: requires the detailed knowledge of the machine's geometry and of the properties of the employed materials, besides software for electromagnetic calculation. It is considered to be the most precise procedure, although costly, and it is employed basically by manufacturers, designers and researchers.

2. Estimation based on steady-state motor models: the parameter values are obtained through the solution of equations derived from state-models employing data from tests, measurements or provided by manufacturers. This class includes the standard testing methods.

3. Frequency-domain parameter estimation: the parameter values are estimated from the transfer function observed during tests. It is not a common industry practice.

4. Time-domain parameter estimation: the parameter values are adjusted so as the response calculated with a system of differential equations fits the observed time response.

5. Real-time parameter estimation: commonly applied to controllers for continuous tuning of parameters of simplified models, compensating parameter variation due to temperature change, saturation and other effects in the machine.

To design the 3 phase induction motor of the stator, rotor, end rings, and main parts of the induction motor is very difficult by using the manual calculation or software. The design of the induction motors is been well established, there are some areas which require special care. The manual design is been a lengthy calculation and if any change in the parameters needs to be recalculated. This results in the time and effort is required by the designer to do the calculations accurately. As an example, after doing the calculations of an induction motor design it is observed that performance of the machine is not satisfactory and dimension of the machine is uneconomical. To solve this, the designer has to change some design parameters like electrical loading, magnetic loading, insulation thickness etc. Hence iterative calculation of the entire design procedure is required to achieve a satisfactory result [5].

2.1. Output Coefficient for Induction Machines

As with all electric machines, the design process begins with the calculation of the output coefficient in the induction motor design. The general formulas for design are given below [6].

To calculate the relationship between the $Dis^2{\cdot}L$ (the standard output coefficient), where stator inner diameter (D_{is}) and stack length (L), and the machine power and performance, we start by calculating the airgap apparent power S_{gap},

$$S_{gap} = 3 \cdot E_1 \cdot I_{1n} \tag{1}$$

Also, the input apparent power S_{1n} is

$$S_{1n} = 3 \cdot V_{1n} \cdot I_{1n} = \frac{P_n}{\eta_n \cdot \cos\varphi_{1n}} \tag{2}$$

where P_n is the rated output power and η_n and $\cos\varphi_{1n}$ are the assigned values of rated efficiency and power factor based on past experience.

The emf E_1 may be written as a function of airgap pole flux.

$$E_1 = 4 \cdot f_1 \cdot K_f \cdot W_1 \cdot K_{w1} \cdot \phi \tag{3}$$

where f_1 is frequency, $1.11 > K_f > 1.02$ form factor (dependent on teeth saturation), W_1 is turns per phase, and K_{w1} is winding factor, $\emptyset$ pole flux.

$$\phi = \alpha_i \cdot \tau \cdot L \cdot B_g \tag{4}$$

where α_i is flux density shape factor dependent on the magnetic saturation coefficient of teeth and B_g is flux density in the airgap. The pole pitch τ is given in Equation (5).

$$\tau = \frac{\pi \cdot D_{is}}{2 \cdot p_1} \tag{5}$$

The number of speed $n_1 = \dfrac{f_1 \cdot 60}{p_1}$ and the air gap apparent power are regulated as follows. Finally, S_{gap} is:

$$S_{gap} = K_f \cdot \alpha_i \cdot K_{w1} \cdot \pi^2 \cdot D_{is}^2 \cdot L \cdot \frac{n_1}{60} \cdot A_1 \cdot B_{av} \tag{6}$$

with A_1 is the specific electrically load (a·c/m):

$$A_1 = \frac{6 \cdot W_1 \cdot I_{1n}}{\pi \cdot D_{is}} \tag{7}$$

where B_{av} the specific magnetic load (T),

$$B_{av} = \frac{\phi}{\alpha_i \cdot \tau \cdot L} \tag{8}$$

We might separate the volume utilization factor C_0 (Esson's constant) as

$$C_0 = k_f \cdot \alpha_i \cdot K_{w1} \cdot \pi^2 \cdot A_1 \cdot B_{av} = \frac{60 \cdot S_{gap}}{D_{is}^2 \cdot L \cdot n_1} \tag{9}$$

C_0 gives energy that can be taken in a minute from the unit volume of the machine. It is a measure of how much you have benefited from the material (kVA·minute/m³) [7].

C_0 is not a constant as both the values of A_1 (a·c/m) and airgap flux density B_{av} increase with machine torque and with the number of pole pairs. The $Dis^2{\cdot}L$ output coefficient may be calculated from (9) with S_{gap} from Equations (1) and (2).

$$D_{is}^2 \cdot L = \frac{1}{C_0} \cdot \frac{60}{n_1} \cdot \frac{K_e \cdot P_n}{\eta_n \cdot \cos\varphi_{1n}} \tag{10}$$

Typical values of C_0 as a function S_{gap} with pole pair p_1 as parameter for low power induction motors is given in Fig. 1.

The $Dis^2{\cdot}L$ output constant (proportional to rotor core volume) is, in fact, almost proportional to machine rated shaft torque. Torque production apparently requires less volume as the pole pairs number p_1 increases, C_0 increases with p_1.

It is standard to assign a value λ to the stack length to pole pitch ratio:

$$\lambda = \frac{L}{\tau} = \frac{2 \cdot L \cdot p_1}{\pi \cdot D_{is}} \quad 0.6 < \lambda < 3.0 \tag{11}$$

The stator bore diameter D_{is} may now be calculated.

$$D_{is} = 3\sqrt{\frac{2 \cdot p_1}{\pi \cdot \lambda} \cdot \frac{1}{C_0} \cdot \frac{p_1}{f_1} \cdot \frac{K_e \cdot P_n}{\eta_n \cdot \cos\varphi_{1n}}} \qquad (12)$$

This is a standard design formula. However, this value is not enough to obtain the total volume of the machine. For this, the stator outer diameter value D_{out} is standardized in most motor designs.

$$D_{out} = \sqrt{\frac{2 \cdot p_1^2}{\pi \cdot \lambda} \cdot \frac{1}{C_0 \cdot f_1} \cdot \frac{K_e \cdot P_n}{\eta_n \cdot \cos\varphi_{1n}} \cdot \frac{1}{D_{is} \cdot f_0(D_{is})}} \qquad (13)$$
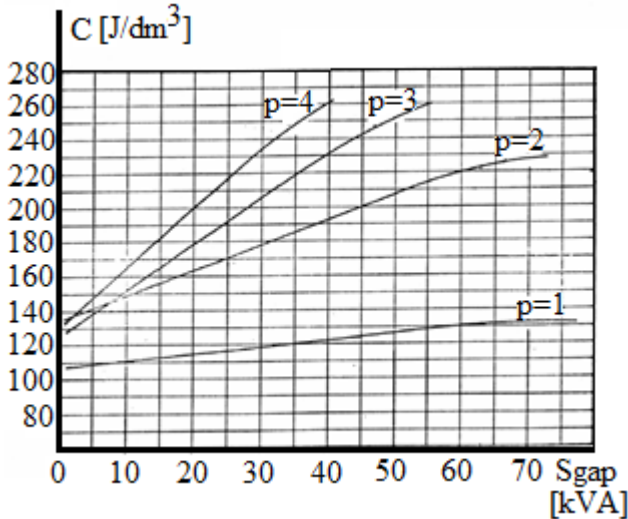
Fig. 1. Esson's constant C_0 versus S_{gap} [6].

After calculating the stator inner diameter of the induction motor, the ratios given in the Table 1 are used to calculate the stator outside diameter. This formulation provides great convenience for motor designers.

Table 1. Inner/outer stator diameter ratio [6]

$2p_1$	2	4	6	8
D_{is}/D_{out}	0.54-058	0.61-0.63	0.68-0.71	0.72-074

After designing the main dimension of the induction motor, stator slot design, rotor slot design, coil design, shaft design, frame design and etc. design are performed. Details of these designs are given in reference [6, 8, 9]. The general cross-section view of the designed motor [10] and the details of the stator and rotor slot structures are given in Figures 2 (a), (b) and (c).
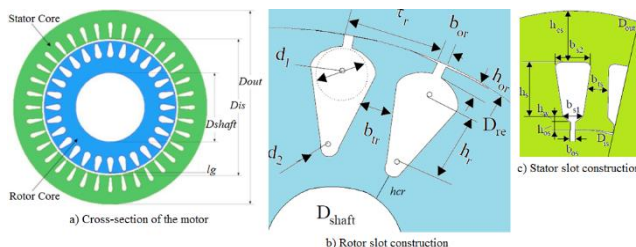

Fig. 2. a) Cross-section of the motor, b) rotor slot construction c) Stator slot construction.

2.2. The Effect of Magnetic and Electrical Loading Coefficients

The first step in the design of rotating electric machines is to obtain the expression $D_{is}^2 \cdot L$. This expression is possible by selecting appropriate values of specific magnetic and specific electrical loading coefficient and this value is proportional to the volume of the machine.

The total magnetic flux value in the machine's air-gap is called total magnetic loading. The average flux density value in the machine's air gap is known as the specific magnetic loading B_{av}. Accordingly, the following expression can be written:

Total magnetic loading = $p_1 \cdot \emptyset$ Wb

The specific magnetic loading can be written as in Equation (14).

$$B_{av} = \frac{p_1 \cdot \phi}{\pi \cdot D_{is} \cdot L} \text{ T} \qquad (14)$$

The sum of the amper and conductors around the stator is called the total electrical loading. The number of amper·conductors per meter of stator circumference in the air-gap is known as the specific electrical loading A_1. Accordingly, the following expression can be written:

Total electrical loading= $I_{1n} \cdot Z$ amper·conductor

The specific electrical loading can be written as in Equation (15).

$$A_1 = \frac{I_{1n} \cdot Z}{\pi \cdot D_{is}} \text{ Amper·conductor/metre} \qquad (15)$$

Change of the specific magnetic loading B_{av} affects the maximum flux density in the iron sections, the magnetizing current, the power factor, the size of the machine, the overload capacity, the stray load losses and the core losses [3, 8, 11].

Change of the specific electrical loading A_1 affects the size of the machine, overload capacity, temperature increase and loss of copper in conductors [3, 11-13].

There are some papers in the literature that the magnetic loading coefficient can be used between 0.3 - 0.65 T and the magnetic electrical loading coefficient can be used between 5000 - 450000 a·c/m [2, 5, 14]. The designer can use these values or use past experience to get approximate values for these coefficients.

The advantages and disadvantages of high specific electrical loading coefficient can be given as [2, 8, 13, 14-18].

Advantages:
- Small motor size
- Lower costs

Disadvantages:
- Higher use of copper
- More copper loss and stray load losses
- Smaller overload capacity
- High temperature increase
- Lower efficiency
- Increased number of conductors and accordingly increased leakage reactance

The advantages and disadvantages of the high specific magnetic loading coefficient can be given as [8, 13, 15, 18-20].

Advantages:
- Small motor size
- Lower costs
- Overload capacity increases

Disadvantages:
- Low power factor
- Low efficiency

2.3. Specifications of the Designed Motor

Designed motor specifications are [6]:
- Rated power: P_n [kW] = 5.5

- Synchronous speed: n_1 [rpm] = 1800
- Line supply voltage: V_1 [V] = 460
- Supply frequency: f_1 [Hz] = 60
- Number of phases: m = 3
- Phase connections: Star
- Targeted power factor: $cos\varphi_{1n}$ = 0.83
- Targeted efficiency: η_n = 0.895
- p.u. locked rotor torque: t_{LR} = 1.75
- p.u. locked rotor current: i_{LR} = 6
- p.u. breakdown torque: t_{bK} = 2.5
- Insulation class: F
- Temperature rise: class B

- Protection degree: IP55 – IC411
- Service factor load: 1.0
- Environment conditions: standard (no derating)

3. Obtained Results And Discussion

The design values obtained by the written Matlab code are given in Table 2. When the results are examined, it is seen that the obtained values support the reference motor values. It shows that written in Matlab code is working correctly. The algorithm for the design process is given in Fig. 18.

Table 2. Obtained motor parameters values from matlab program

Parameters	Variables	Unit	Reference Values [6]	Obtained Values
Apparent Airgap Power	Sgap	VA	7181.8	7181.8
Stator Bore Diameter	Dis	m	0.1116	0.1114
Stack Length	L	m	0.1315	0.13124
Pole Pitch	to	m	0.0876	0.087491
Stator Slot Pitch	tos	m	9.734 10^{-3}	9.7212 10^{-3}
Stator Outer Diameter	Dout	m	0.18	0.17967
Airgap Length	g	m	0.3111 10^{-3}	0.31182 10^{-3}
Stator Slot Number	Ns		36	36
The Zone Factor	Kq1		0.9598	0.9598
The Chording Factor	Ky1		0.9397	0.9397
Stator Winding Factor	Kw1		0.9019	0.9019
The Pole Flux	fi	Wb	5.878 10^{-3}	5.8592 10^{-3}
Number Of Turns Per Phase	W1	turns/phase	186.8	187.21
Number Of Conductors Per Slot	ns	turns/slot	31.33	31.2
Airgap Flux Density	Bg	T	0.726	0.728
Rated Current	I1n	A	9.303	9.2927
Magnetic Wire Cross Section	Aco	m^2	2.6733 10^{-6}	2.0651 10^{-6}
Magnetic Wire Diameter	dco	m	1.622 10^{-3}	1.6215 10^{-3}
Stator Slot Sizing				
Useful Slot Area	Asu	m^2	155.7 10^{-6}	154.88 10^{-6}
Stator Tooth Width	bts	m	4.75 10^{-3}	4.7563 10^{-3}
Stator Slot Lower Width	bs1	m	5.42 10^{-3}	5.4012 10^{-3}
Stator Slot Upper Width	bs2	m	9.16 10^{-3}	9.1309 10^{-3}
Stator Slot Useful Height	hs	m	21.36 10^{-3}	21.315 10^{-3}
Airgap mmf	Fmg	Aturns	242.77	243.45
Stator Tooth mmf	Fmts	Aturns	41.99	41.915
Rotor Tooth mmf	Fmtr	Aturns	55.11	55.465
Stator Back Iron Height	hcs	m	10.34 10^{-3}	10.322 10^{-3}
Back Core Flux Density	Bcs	T	1.456	1.4549
Rotor Slots Sizing				
Rotor Slot Area	Ab	m^2	81.65 10^{-6}	81.67 10^{-6}
Rotor Slot Pitch	tor	m	12.436 10^{-3}	12.429 10^{-3}
Rotor Tooth Width	Btr	m	5.88 10^{-3}	5.8909 10^{-3}
Rotor Slot Upper Width	d1	m	5.70 10^{-3}	5.7696 10^{-3}
Rotor Slot Lower Width	d2	m	1.2 10^{-3}	1.697 10^{-3}
Rotor Slot Height	hr	m	20 10^{-3}	18.07 10^{-3}
Rotor Back Core Height	hcr	m	13.55 10^{-3}	13.529 10^{-3}
Shaft Diameter	dshaft	m	35.9 10^{-3}	39.032 10^{-3}
Nominal Torque	Ten	N.m	29.77	29.774
End Ring Depth	bb	m	24.445 10^{-3}	24.533 10^{-3}
End Ring Length	aa	m	10.02 10^{-3}	9.9734 10^{-3}
The Magnetization Current				
Stator Back Core mmf	Fmcs	Aturns	54.22	57.803
Rotor Back Core mmf	Fmcr	Atırns	32.4	42.303
Total mmf	F1m	Aturns	853.68	880.67
Magnetization Current	Imu	A	3.86	4.0169
Resistances and Inductances				
Stator Phase Resistance	Rs	ohm	0.468375	0.46808
Rotor Cage Resistance Reduced To The Stator	RrS1	ohm	1.1295	1.1512
Stator Phase Leakage Reactance	Xs1	ohm	2.17	2.1937
Equivalent Rotor Bar Leakage Reactance	Xbe	ohm	3.1877 10^{-4}	3.2123 10^{-4}
Rotor Leakage Reactance	Xr1	ohm	3.6506	3.6284
Rotor Resistance	RrSn	ohm	0.709	0.84353
Equivalent Rotor Leakage Reactance	Xr1Sn	ohm	3.938	2.418
Magnetization Reactance	Xm	ohm	66.70	63.921
Losses and Efficiency				
Stator Winding Losses	Pcus	W	121.607	121.26
Rotor Cage Losses	Pcur	W	137.417	163.13
Stator Tooth Weight	Gt1	Kg	4.168	4.0072
Stator Teeth Fundamental Losses	pt1	W	36.45	36.376
Yoke Weight	Gy1	Kg	5.877	5.7154

Stator Back Iron Fundamental Losses	$py1$	W	45.145	43.951
Fundamental Iron Losses	$Piron1$	W	81.595	80.327
Rotor Teeth Weight	Gtr	Kg	3.749	3.5341
Tooth Flux Pulsation Core Loss	$Pirons$	W	7.24	6.9292
Total Core Loss	$piron$	W	88.835	87.256
Total Losses	$Ptopkay$	W	468.859	492.65
Efficiency	$verim$		92.14	91.779

After the design process has been completed, the values of B_{av}, A_1 and C_0 are calculated using Equations (14) and (15). The comparison of the selected values at the beginning of the design procedure with the calculated values are given in Table 3. When the results are examined, it is seen that all three obtained values are close to each other.

Table 3. Comparison of B_{av}, A_1 and C_0

Parameters	Chosen	Calculated	% Difference
B_{av}	0.67	0.7	4.47 %
A_1	30300	29825	-1.56 %
C_0	147000	146980	-0.013 %

3.1. Change of the B_{av}

In this case, the specific electrical loading coefficient A_1 is kept constant at 30300 (a·c/m), and the specific magnetic loading coefficient B_{av} is increased from 0.3 (T) to 0.8 (T). The obtained results are given in Figs. 3-7.
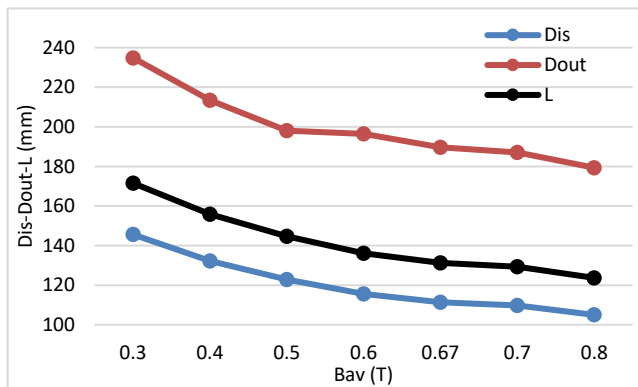
Fig. 3. Change of B_{av} and D_{is}, D_{out}, L.
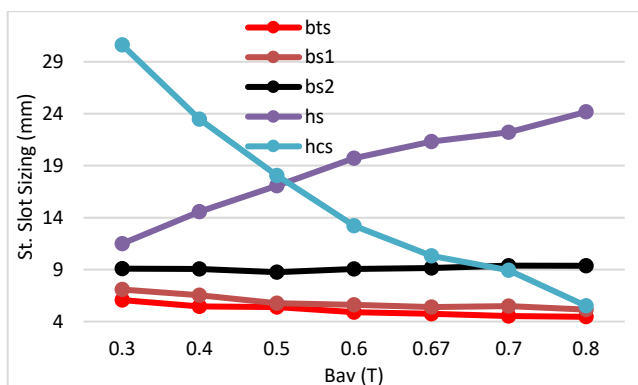
Fig. 4. Change of B_{av} and stator slot sizing.
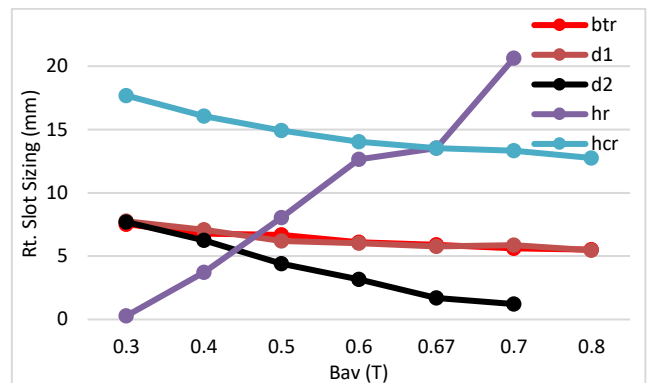
Fig. 5. Change of B_{av} and rotor slot sizing.
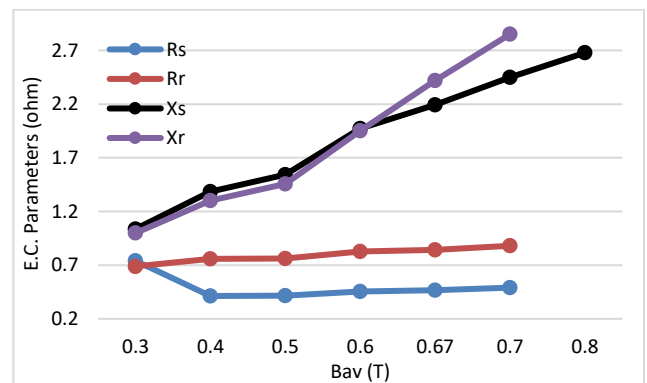
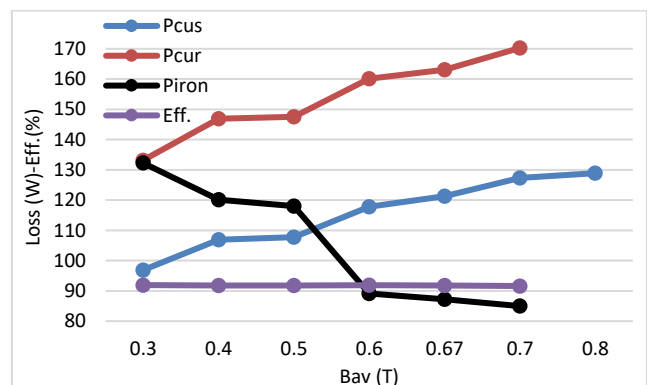**Fig. 6.** Change of B_{av} and equivalent circuit parameters.

Fig. 7. Change of B_{av} and losses, efficiency.

Due to the increase of the specific magnetic load coefficient, a decrease in the motor dimensions has occurred. The reduction in outer diameter, caused a reduction in the height of the stator back core. This has resulted in an increase in the value of back core flux density. Stator and rotor slot sizes have also changed. A certain amount of increase in reactance and resistance values has occurred. The decrease in motor size results in a decrease in core weight. Despite the increase in magnetic flux density values, iron losses are reduced. The increase in the used number of conductors resulted in an increase in copper losses.

3.2. Change of the A_1

In this case, the specific magnetic loading coefficient is kept constant at 0.67 (T), and the specific electrical loading coefficient A_1 (a.c/m) is increased from 10000 to 35000. The obtained results are shown in Figs. 8-12.
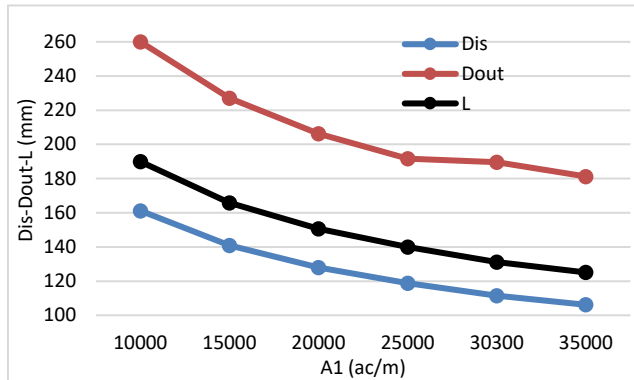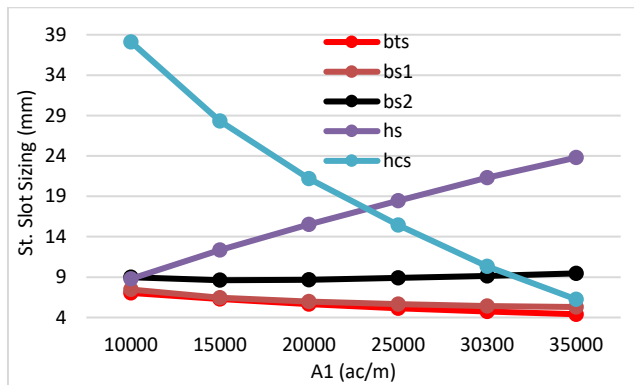

Fig. 8. Change of A_1 and D_{is}, D_{out}, L.
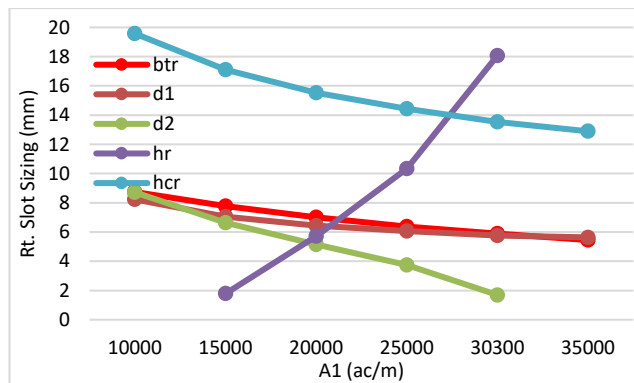

Fig. 9. Change of A_1 and stator slot sizing.
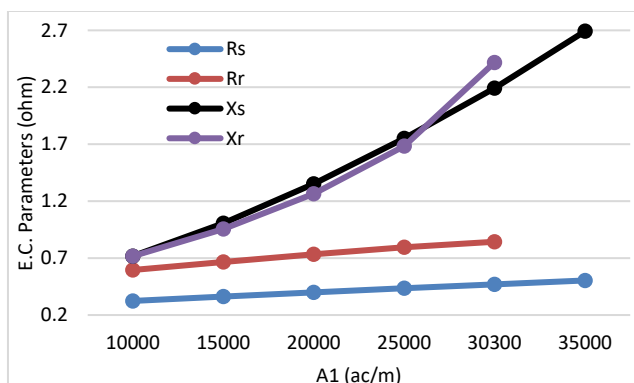

Fig. 10. Change of A_1 and rotor slot sizing.
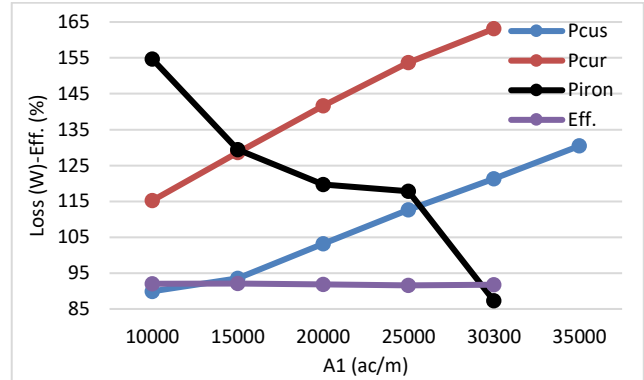

Fig. 11. Change of A_1 and equivalent circuit parameters.

Fig. 12. Change of A_1 and losses, efficiency.

The increase in the value of the electrical loading coefficient led to a decrease in the motor outer diameter, inner diameter and package length. This has also caused changes in the stator and rotor slot values of the motor.

In addition, the number of windings has increased in order to be able to provide the required amper·conductor number. This is led to an increase in copper loss.

It is seen that the equivalent circuit parameters also increase due to the increase of the number of windings. Core losses have led to a great decline in the case of decline in motor size and the decrease in core weight. Efficiency value is almost the same.

3.3. Change of the B_{av} and A_1

In this case, both the specific magnetic loading coefficient B_{av} value and the specific electrical loading coefficient A_1 value are increased. The results obtained are shown in Figs. 13-17.
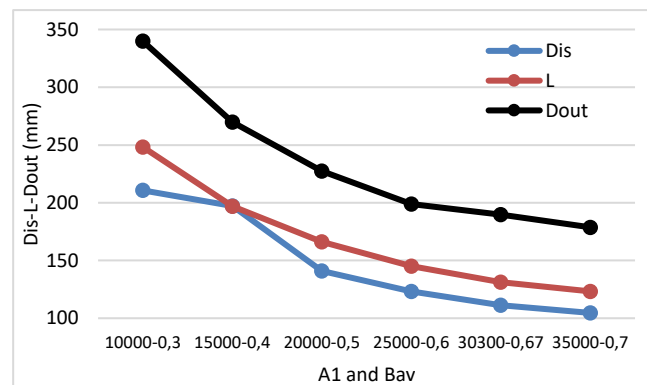

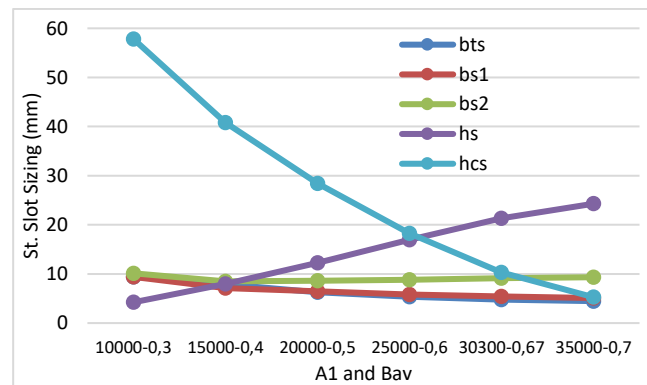**Fig. 13.** Change of B_{av}, A_1 and D_{is}, D_{out}, L.

Fig. 14. Change of B_{av}, A_1 and stator slot sizing.
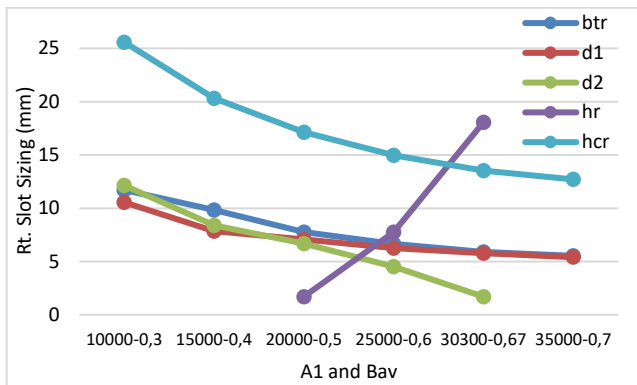
Fig. 15. Change of B_{av}, A_1 and rotor slot sizing.
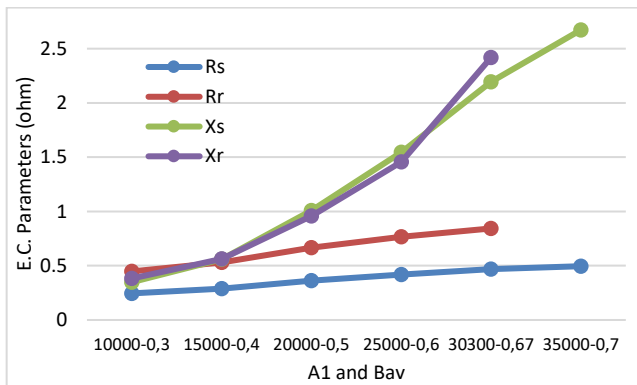

Fig. 16. Change of B_{av}, A_1 and equivalent circuit parameters.
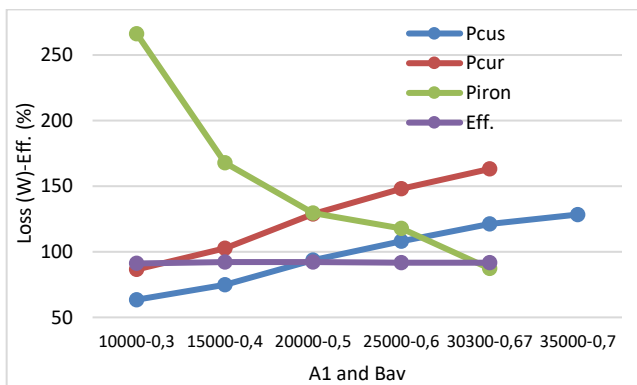

Fig. 17. Change of B_{av}, A_1 and losses, efficiency.

When the graphs obtained by increasing both the specific magnetic loading and the specific electrical loading coefficients are examined, it is seen that there are similar graphs to the changes of the B_{av} and A_1.

4. Conclusion

In this study, the design process is given for 5.5 kW squirrel cage induction motor, and design results are obtained by software written in MATLAB. It was seen that the obtained result is consistent with the value of the reference motor. In the second part of the study, the design effects were investigated by changing the specific magnetic loading and the specific electrical loading coefficients which affect the output coefficient (C_0) for the target efficiency. It has been shown that it is possible to design a more efficient but cost effective or less efficient but cheaper motor using the specified design principles and software. In the study, it has been shown that the cost can be reduced by targeting the reference motor.
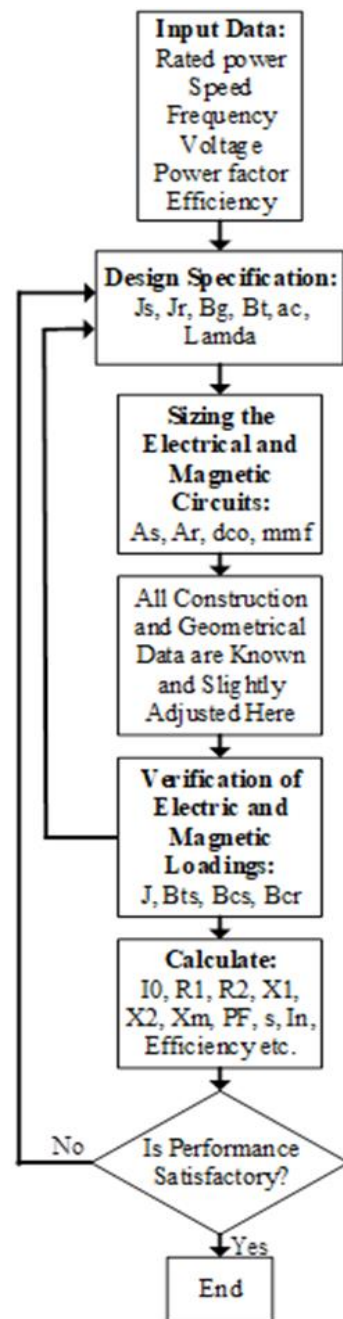

Fig. 18. Design algorithm of the induction motor [6, 21].

References

[1] O. Akman, and A. Ürkmez, "Asenkron motor tasarımının bilgisayar programı ile gerçekleştirilmesi," *presented at the ELECO*, Bursa, Türkiye, Dec. 8-12, 2004, pp. 1-3.

[2] Design Modification of Induction Motor for Propulsion Purposes, Chapter 7, pp. 128-155.

[3] P. S. Parmar and Mr. K. Limbachiya, "Design and optimisation of 3-Phase induction motor," *presented at the Recent Trends in Electrical and Electronics & Communication Engineering*, Vadodara, India, Apr. 17–18, 2015, pp. 53-57.

[4] C. A. C. Wengerkievicz, R. A. Elias, N. J. Batistela, N. Sadowski, P. Kuo-Peng, S. C. Lima, P. A. Silva, A. Y. Beltrame, "Estimation of three-phase induction motor equivalent circuit parameters from manufacturer catalog data," *J. Microwaves Optoelectron. Electromagn. Appl.*, vol. 16, no. 1, pp. 90-107, Mar. 2017, 10.1590/2179-10742017v16i1873.

[5] B. Somashekar, "Design of three phase induction motor using matlab programming," *Int. J. Recent Innovation Trends Comput. Commun.*, vol. 3, no. 8, pp. 5188-5193, Aug. 2015.

[6] I. Boldea, and S. A. Nasar, The Induction Machine Handbook, Crc Press, Washington, D.C., 2002, pp. 1-35.

[7]   E. Gürleyen, Orta Güçlü Sincap Kafesli Asenkron Motor Tasarım Programı Geliştirilmesi, İstanbul Teknik Üniversitesi Fen Bilimleri Enstitüsü, Yüksek Lisans Tezi, Haziran 2013, pp. 93.

[8]   O. Gürdal, Elektrik Makinalarının Tasarımı, Bursa Orhangazi Üniversitesi Yayınları, Bursa, 2015, pp. 535.

[9]   K. M. V. Murthy, Computer-Aided Design of Electrical Machines, BS Publications, Hyderabad, 2008, P 335.

[10]   Y. L. Karnavas, and I. D. Chasiotis, "Influence of soft magnetic materials application to squirrel cage induction motor design and performance," Eng. J., vol. 21, no. 1, pp. 193-206, Jan. 2017, 10.4186/ej.2017.21.1.19.

[11]   Z. Fazlipour, R. Kianinezhad, and M. Razaz, "Genetic algorithm based design optimization of a six phase induction motor," J. *Electr. Eng. Technol.*, vol. 10, no. 3, pp. 1007-1014, 2015, 10.5370/JEET.2015.10.3.1007.

[12]   P. A. Sakpal, and V. Mohale, "Design and analysis of a premium efficiency (IE3) induction motor," *Int. J. Res. Eng. Technol.*, vol. 5, no. 2, pp. 198-203, Feb. 2016.

[13]   Design of Induction Motor, p. 46.

[14]   J. Singh, K. Singh, and H. Kaur, "Designing of three phase squirrel cage induction motor for good efficiency," *Int. J. Eng. Innovative Technol.*, vol. 5, no. 7, pp. 40-45, Jan. 2016.

[15]   A. Nanoty, Induction Motors, 2014, p. 67.

[16]   Three Phase Induction Motors, prepared by :-8th _EE GECD, p. 7.

[17]   http://www.navodayaengg.in/wp-content/uploads/2016/02/Lesson-42-Specific-Loadings..docx.

[18]   F. Oladipo, O. O. Temitayo, and O. F. Eziafa, "Analysis of the effect of electric and magnetic loadings on the design parameters of an induction motor and its performance using matlab/simulink," *Int. J. Eng. Res. Appl.*, vol. 5, no. 3, pp. 38-43, Mar. 2015.

[19]   D. Sharma, R. K. Saini, and S. Pathania, "Design, analysis and selection of electric and magnetic loading for different rating of squirrel cage induction motors by using matlab gui software," *Int. J. Innovative Res. Elec. Electron. Instrum. Control Eng.*, vol. 3, no. 4, pp. 20-22, Apr. 2015, 10.17148/IJIREEICE.2015.3418.

[20]   V. P. Mini, and S. Ushakumari, "Rotor fault detection and diagnosis of induction motor using fuzzy logic," *Amse J. Modell. A.*, vol. 87, no. 2, pp. 19-40, Apr. 2014.

[21]   V. de P. B. Aguiar, R. S. The Pontes, and T. R. F. Neto, "Three-phase induction motor preliminar design assisted by CAD software based on Brazilian Standards," pp 1-11.